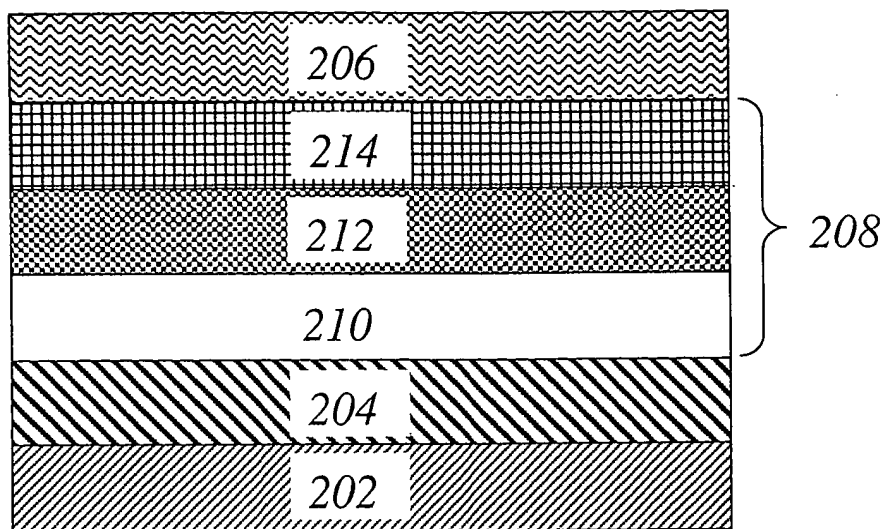
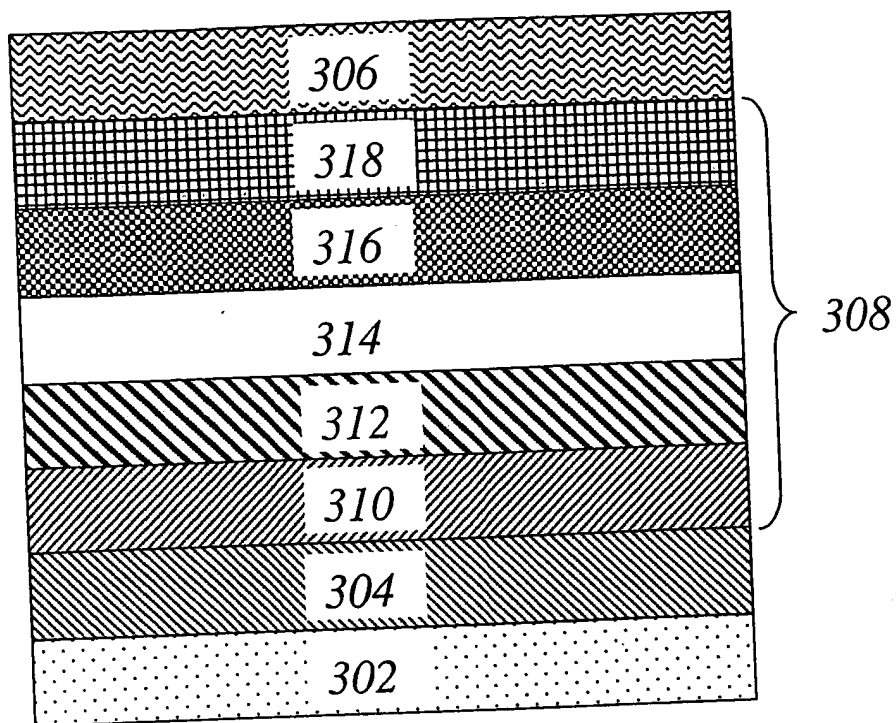


FIGS. 1. Schematic diagrams of the two-layer structures of preferred EL devices



FIGS. 2. Schematic diagrams of the three-layer structures of preferred EL devices



FIGS. 3. Schematic diagrams of the multi-layer structures of preferred EL devices

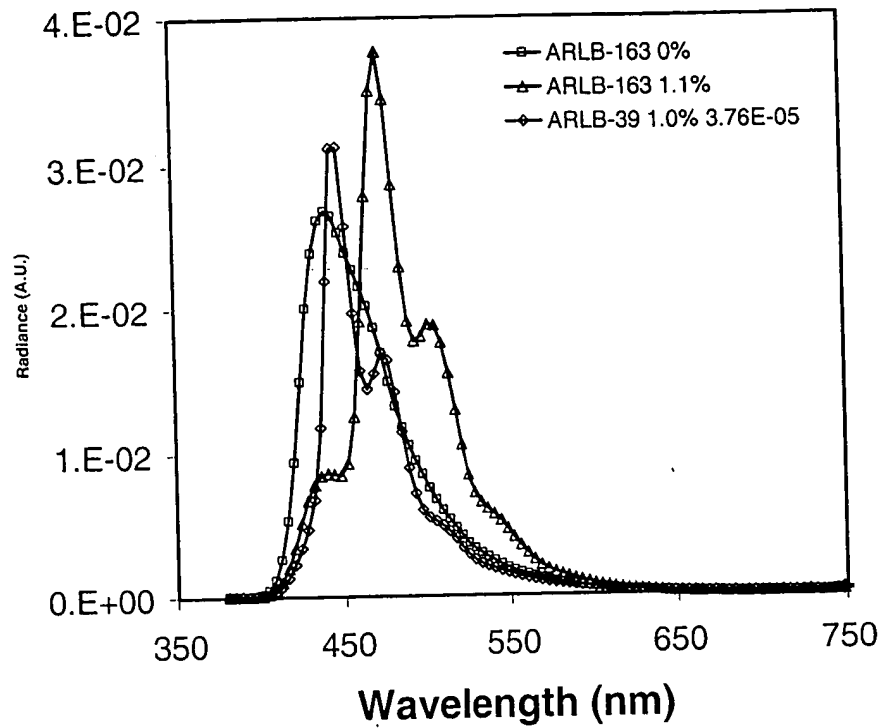


Fig. 4 EL spectra for undoped TBADN (Example 16) TBADN doped with ARL-39 (Example 17) at a concentration of 1.1%, and TBADN doped with ARL-163 (Example 18) at a concentration of 1.0%. The EL spectra were measured at a drive current density of 20mA/cm<sup>2</sup>.

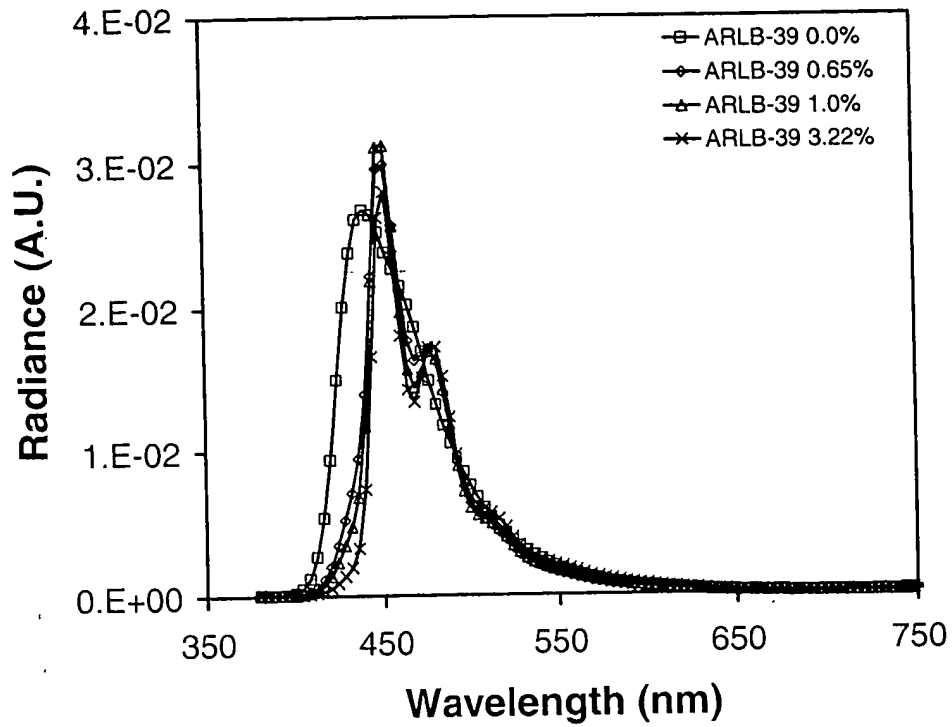


Fig. 5 Spectra for ARLB-39 as a function of doping concentration measured at a drive current density of 20 mA/cm<sup>2</sup>

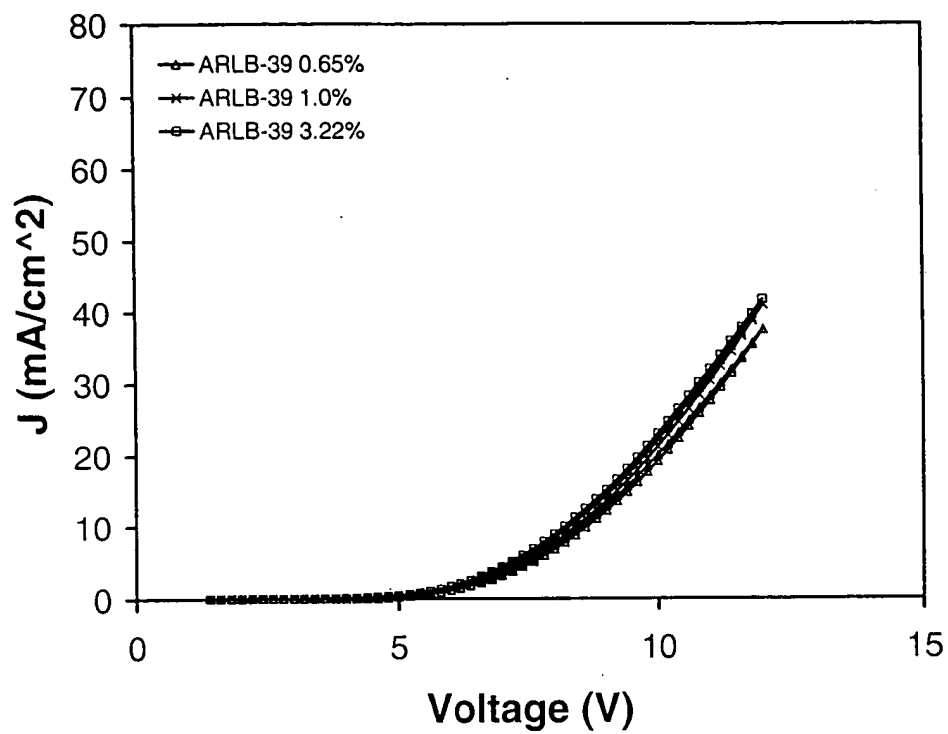


Fig. 6 illustrated the current density – voltage relation as a function of three doping concentration

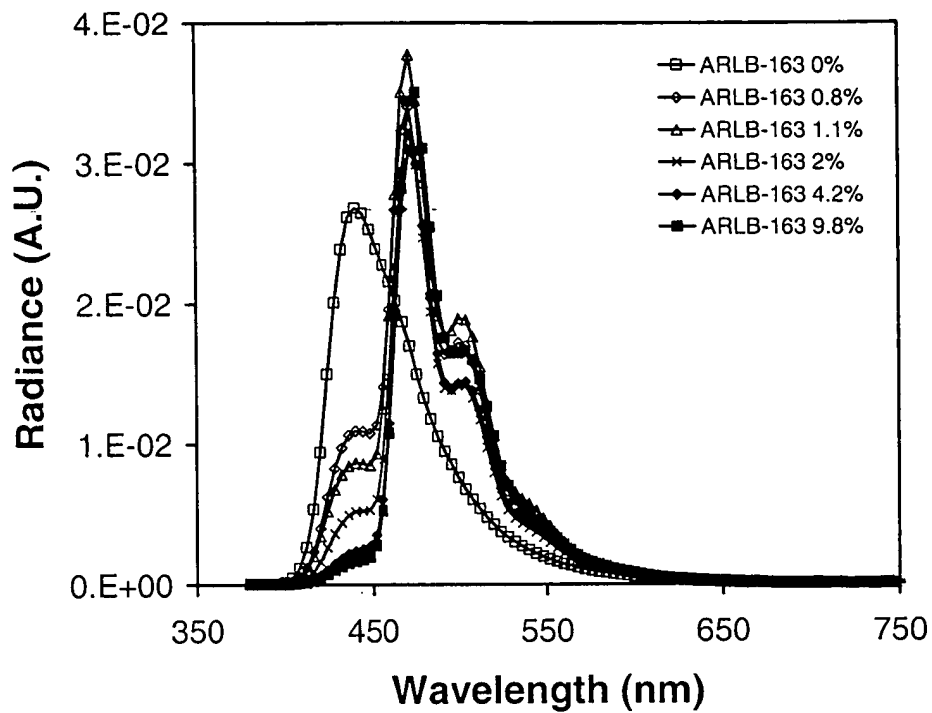


Fig. 7 Spectra for ARLB-39 as a function of doping concentration measured at a drive current density of 20 mA/cm<sup>2</sup>

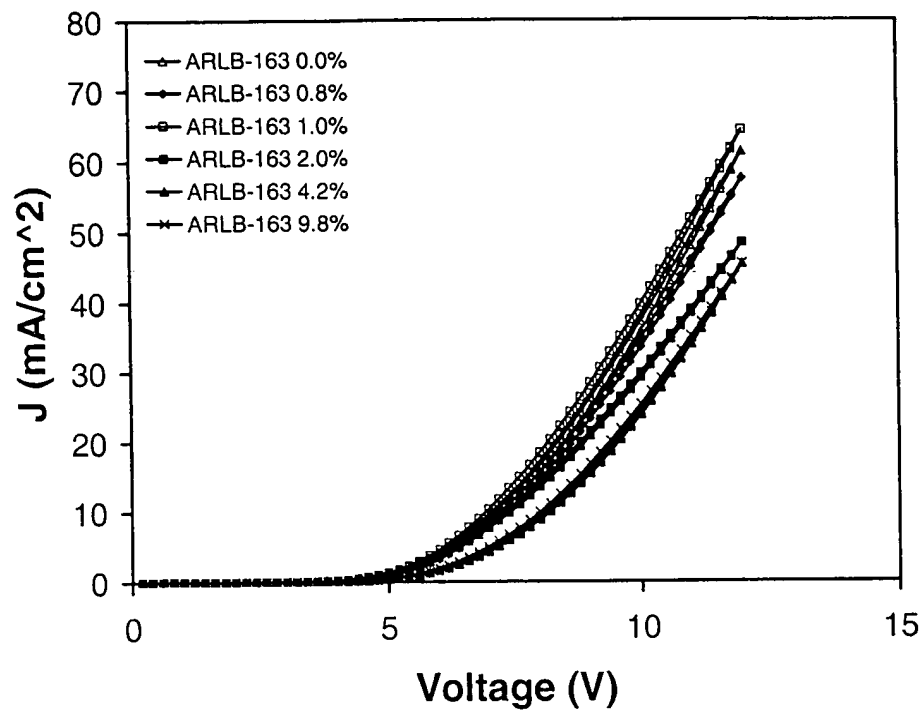


Fig. 8 illustrated the current density – voltage relation as a function of doping concentration.



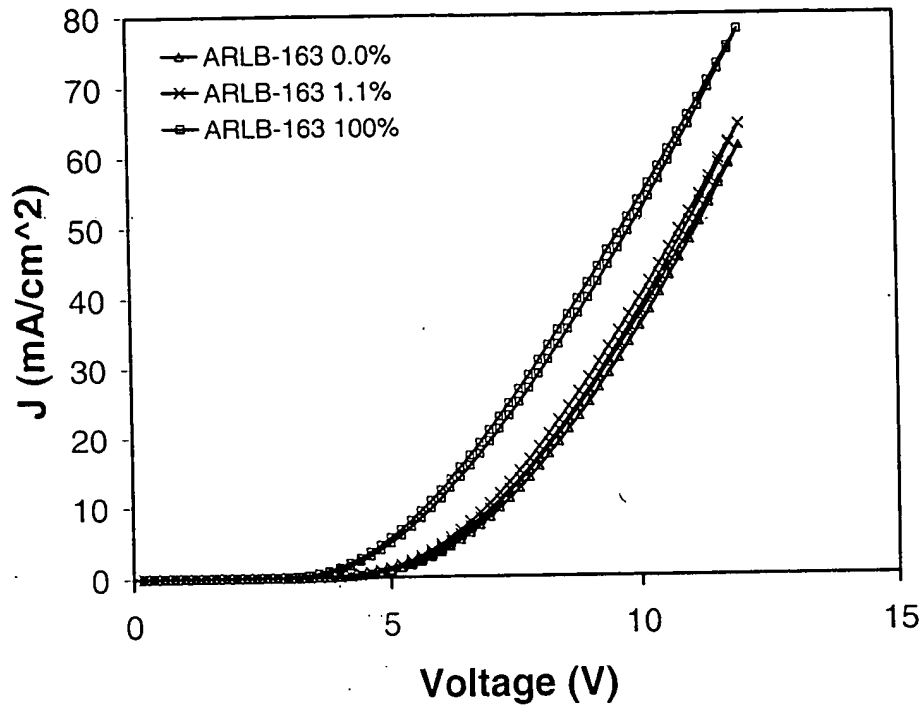


Fig. 9 illustrated the current density – voltage relation for undoped TBADN layer, TBADN doped with 1.1% (v/v) ARLB-163 and 1000 (Å) thick ARLB-163 with no doping